Variable splitting ratio 2×2 MMI couplers using multimode waveguide holograms

Shuo-Yen Tseng, Canek Fuentes-Hernandez, Daniel Owens, and Bernard Kippelen

Center for Organic Photonics and Electronics,
School of Electrical and Computer Engineering,
Georgia Institute of Technology, Atlanta, GA 30332

sytseng@gatech.edu

Abstract: Variable power splitting ratio 2×2 MMI couplers using multimode waveguide holograms are analyzed. Theoretical analysis shows that variable splitting ratios can be obtained with surface relief holograms on MMI couplers with fixed dimensions. Devices with paired-imaging lengths are designed on a silicon-on-insulator (SOI) platform. Beam propagation simulations are used to verify a matrix theory analysis and to investigate proposed device performance. Fabrication tolerance of the proposed device is also analyzed.

OCIS codes: (130.3120) Integrated optics devices; (130.2790) Guided waves; (090.1760) Computer holography.

References and links

1. L. B. Soldano and E. C. M. Pennings, "Optical multi-mode interference devices based on self-imaging: principles and applications," J. Lightwave Technol. **13**, 615-627 (1995).
2. P. A. Besse, M. Bachmann, H. Melchior, L. B. Soldano, and M. K. Smit, "Optical bandwidth and fabrication tolerances of multimode interference couplers," J. Lightwave Technol. **12**, 1001-1009 (1994).
3. M. Bachmann, P. A. Besse, and H. Melchior, "Overlapping-image multimode interference couplers with a reduced number of self-images for uniform and nonuniform power splitting," Appl. Opt. **34**, 6898-6910 (1995).
4. P. A. Besse, E. Gini, M. Bachmann, and H. Melchior, "New 2×2 and 1×3 multimode interference couplers with free selection of power splitting ratios," J. Lightwave Technol. **14**, 2286-2293 (1996).
5. D. S. Levy, Y. M. Li, R. Scarmozzino, R. M. Osgood Jr., "A multimode interference-based variable power splitter in GaAs-AlGaAs," IEEE Photon. Technol. Lett. **9**, 1373-1375 (1997).
6. D. J. Y. Feng, T. S. Lay, and T. Y. Chang, "Waveguide couplers with new power splitting ratios made possible by cascading of short multimode interference sections," Opt. Express **15**, 1588-1593 (2007), http://www.opticsinfobase.org/abstract.cfm?URI=oe-15-4-1588
7. S.-Y. Tseng, Y. Kim, C. J. K. Richardson, and J. Goldhar, "Implementation of discrete unitary transformations by multimode waveguide holograms," Appl. Opt. **45**, 4864-4872 (2006).
8. H. Wei, J. Yu, Z. Liu, X. Zhang, W. Shi, and C. Fang, "Fabrication of 4×4 tapered MMI coupler with large cross section," IEEE Photon. Technol. Lett. **13**, 466-468 (2001).
9. J. M. Heaton and R. M. Jenkins, "General matrix theory of self-imaging in multimode interference (MMI) couplers," IEEE Photon. Technol. Lett. **11**, 212-214 (1999).
10. K. Solehmainen, M. Kapulainen, M. Harjanne, and T. Aalto, "Adiabatic and multimode interference couplers on silicon-on-insulator," IEEE Photon. Technol. Lett. **18**, 2287-2289 (2006).
11. T. Tsuchizawa, K. Yamada, H. Fukuda, T. Watanabe, J. Takahashi, M. Takahashi, T. Shoji, E. Tamechika, S. Itabashi, and H. Morita, "Microphotonics devices based on silicon microfabrication technology," IEEE J. Sel. Top. Quantum Electron. **11**, 232-240 (2005).
12. G. R. Hadley, "Wide-angle beam propagation using Pade approximant operators," Opt. Lett **17**, 1426-1428 (1992).

#82652 - $15.00 USD Received 2 May 2007; revised 28 Jun 2007; accepted 29 Jun 2007; published 6 Jul 2007

13. K. Kawano and T. Kiton, *Introduction to Optical Waveguide Analysis* (Wiley, New York, 2001).
14. Optical Modesolver, Photonics Research Laboratory, University of Maryland, MD (2006), http://www.photonics.umd.edu/software/modesolver.zip

1. Introduction

Power splitters are important building blocks in integrated photonics. Multimode interference (MMI) couplers [1] are particularly attractive for power splitter applications because of their large fabrication tolerance, large bandwidth, and compact size [2]. For traditional 2×2 MMI power splitters, only limited splitting ratios can be achieved using the imaging properties of MMIs [3]. A free choice of power splitting ratio can be achieved with butterfly MMIs [4] or bent MMIs [5] by phase shifts from geometrical variations. However, it could be difficult to cascade these angled or bent devices with other components in integrated optical circuits. Another recently demonstrated approach is to cascade MMIs of different widths to achieve new power splitting ratios [6]. This approach relies on changing the device dimension and geometry to obtain the new splitting ratios. All these approaches require different device dimensions or geometries for different splitting ratios, which could result in potential design difficulties when new splitting ratios are required in existing layouts. A power splitter with fixed device geometry for various splitting ratios is highly desirable in terms of compatibility and ease of integration.

In a recent work [7], it was demonstrated that unitary transformations can be implemented with multimode waveguide holograms. By etching shallow surface relief patterns on the multimode section of an MMI, arbitrary unitary transformations can be implemented with holograms without changing its geometry. In this work, we extend the concept of hologram design by eigenmodes at self-imaging planes [7] to include eigenmodes at paired-imaging planes for the hologram calculation. Using a matrix theory, 2×2 couplers with variable power splitting ratios are designed on a silicon-on-insulator (SOI) [8] platform for its compatibility and ease of integration with the silicon CMOS technology. Beam propagation modeling is used to verify the design concept and investigate the performance of designed devices.

2. Matrix theory of hologram in MMI power splitters at paired-imaging length

Figure 1 shows the schematic of 2×2 MMI power splitters considered in this work. The length L of the multimode section is at half the beat length, L_π [1]:

$$L_\pi = \frac{4 n_c W_e^2}{3\lambda}, \tag{1}$$

where n_c is the core effective index, W_e is the effective width [1] of the multimode section, and λ is the wavelength. By placing the access waveguides at $\pm W_e/6$ from the center of the multimode section, selected modes are excited to produce a paired-image at the 3dB length of $L_\pi/2$ [1]. For the electric field in a single input waveguide, a paired image of equal amplitude and a phase difference of $\pi/2$ is formed at the output bar and cross waveguides. Without a hologram, the MMI functions as a power splitter with 50:50 splitting ratio.

The hologram is in the form of surface relief patterns on top of the multimode section to provide effective index modulation Δn at different parts of the multimode section. Magnitude of Δn can be varied by changing the depth of the surface relief patterns [7]. It was pointed out in Ref.[7] that eigenmodes at self-imaging planes [9] can be used to calculate holograms for unitary matrix-vector multiplications. The interference pattern between the ith and the jth eigenmodes corresponds to the ijth element in matrix $\mathbf{K}$, which relates input vector $\mathbf{V}_i$ and output vector $\mathbf{V}_o$ through unitary matrix-vector multiplication as

$$\mathbf{V}_o = \exp(-i\mathbf{K}L_H)\mathbf{V}_i, \tag{2}$$

#82652 - $15.00 USD Received 2 May 2007; revised 28 Jun 2007; accepted 29 Jun 2007; published 6 Jul 2007

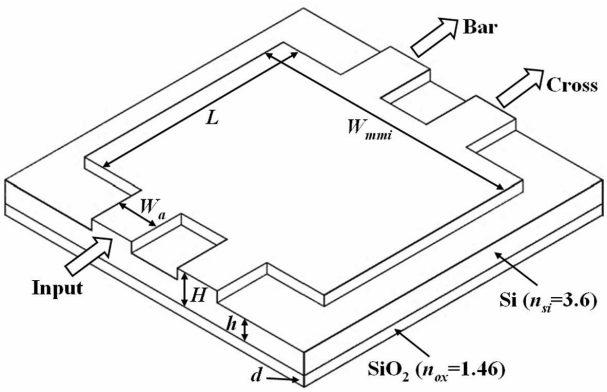

Fig. 1. Schematic of 2×2 MMI power splitter based on silicon-on-insulator (SOI) rib structure.

where L_H is the length of the hologram.

Here, we further extend the theory by using eigenmodes at paired-imaging planes for hologram calculation. At the power splitter input, two eigenvectors $\mathbf{e}_a$=[1,0]^T and $\mathbf{e}_b$=[0,1]^T can be used to represent the complex electric field amplitudes in the input waveguides. When there is no hologram, the transfer matrix **T** representing the MMI is

$$\mathbf{T} = \frac{1}{\sqrt{2}} \begin{bmatrix} 1 & i \\ i & 1 \end{bmatrix}. \tag{3}$$

At the paired imaging plane, we define two new eigenvectors $\mathbf{E}_a = (1/2)^{1/2}[1,i]^T$ and $\mathbf{E}_b = (1/2)^{1/2}[i,1]^T$ to represent the complex electric field amplitudes in the output waveguides. As a result, the MMI represents an identity matrix **I** mapping the input eignevectors $\mathbf{e}_{a,b}$ to the output eigenvectors $\mathbf{E}_{a,b}$. Vectors spanned by $\mathbf{E}_{a,b}$ are related to vectors spanned by $\mathbf{e}_{a,b}$ via basis rotation as

$$\mathbf{V_e} = \mathbf{T}\mathbf{V_E}. \tag{4}$$

We design the hologram by calculating the interference pattern of the two input eigenvectors in the multimode waveguide. The hologram loaded MMI can be represented in matrix form relating input and output vectors as

$$\mathbf{V_E}(L) = \exp(-i\mathbf{K}L_H)\mathbf{V_e}(0) = \mathbf{H}\mathbf{V_e}(0) \tag{5}$$

(note that different bases are used for input and output vectors). **K** is a Hermitian matrix representing the hologram as

$$\mathbf{K} = \begin{bmatrix} 0 & \kappa \\ \kappa & 0 \end{bmatrix}, \tag{6}$$

where κ is a real number representing the coupling coefficient, its magnitude is on the order of $(2\pi/\lambda)(\Delta n/n_c)$ [7], and a common phase factor on the diagonal is ignored for clarity. Using Eq.(4)-Eq.(6), the output field amplitudes in both output ports are thus related to input ports by

$$\mathbf{V_e}(L) = \mathbf{T}\mathbf{H}\mathbf{V_e}(0) = \frac{1}{\sqrt{2}} \begin{bmatrix} \cos\kappa L_H + \sin\kappa L_H & i(\cos\kappa L_H - \sin\kappa L_H) \\ i(\cos\kappa L_H - \sin\kappa L_H) & \cos\kappa L_H + \sin\kappa L_H \end{bmatrix} \mathbf{V_e}(0). \tag{7}$$

For a single input port, the output power at bar and cross ports is thus

$$\text{bar:} \frac{1}{2}(1 + \sin 2\kappa L_H) \tag{8}$$

#82652 - $15.00 USD Received 2 May 2007; revised 28 Jun 2007; accepted 29 Jun 2007; published 6 Jul 2007

$$\text{cross:}\frac{1}{2}(1-\sin 2\kappa L_H). \tag{9}$$

From Eq.(8) and Eq.(9), it is obvious that an arbitrary power splitting ratio can be obtained by varying κ via index modulation Δn or by varying hologram length L_H, while maintaining the dimensions of the MMI.

3. Device design

In this study, an SOI rib waveguide structure [10] with larger mode cross section as compared to the nanowire structure [11] is chosen for its lower coupling loss to optical fibers. The proposed design parameters for the SOI-based MMI in Fig. 1 are chosen as follows: the waveguide height H is 3μm, the slab height h is 2μm, the buried oxide layer thickness d is 1μm, the width of access waveguides W_a is 4μm, the width of the multimode section W_{mmi} is 24μm, the length L of the multimode section is 1080μm, the centers of access waveguides are placed $\pm 4.3\mu$m from the center of the multimode section for paired-imaging. The placement of access waveguides is chosen by approximating the effective width W_e of MMI by taking into account the lateral penetration of the fundamental mode into the cladding as in Ref. [1]. Refractive indices are n_a=1.0(air), n_{si}=3.6, and n_{ox}=1.46. The device is optimized for 1550nm input wavelength and TE polarization.

A 2D wide-angle beam propagation method (WA-BPM) [12] based model is used for device design and simulation. The 3D waveguide structure is converted to a 2D structure using the effective index method [13]. The imaging properties of MMI structures are based on the quadratic dependence between the mode effective indices and the mode numbers. To validate the effective index calculation, the calculated mode effective indices are compared with effective indices calculated with a full vectorial 3D mode solver [14]. The results show a good agreement between the 2D approximation and the full vectorial solution. We expect the 2D WA-BPM calculation to be a very good approximation of the 3D structure.

The hologram is calculated using WA-BPM by propagating equal amplitude and in-phase inputs in the MMI as shown in Fig. 2. In device fabrication, the calculated pattern can be converted to a binary mask and transferred to the surface of the multimode section [7]; the etching depth d_{etch} of the surface relief hologram pattern is directly related to the magnitude of effective index modulation Δn and can be estimated by the effective index method [13]. For this particular design, we calculated the effective index n of the multimode section as a function of the waveguide height h using the effective index method and found Δn and d_{etch} (the variation in waveguide height, Δh) follow an almost linear relation with a slope of $\Delta n/d_{etch} = -7\times 10^{-6}$/nm. By varying d_{etch}, the splitting ratio can be varied through coupling coefficient κ as shown in Eq.(8) and (9). For a fixed d_{etch}, the splitting ratio can be varied by changing the length of the hologram L_H on the multimode section.

4. Device simulation

WA-BPM simulations are used to verify the matrix theory analysis in section 2 and to investigate the performance of the proposed device. In the simulations presented below, the interference pattern in the multimode section in Fig. 2 is used as a perturbation to the core effective index. The hologram features are discretized into $1\mu m \times 1\mu m$ pixels in the simulation.

4.1. Variable power splitting ratio

The dependence of the device power splitting ratio on the coupling coefficient κ is investigated by varying the index modulation Δn using an input wavelength of 1550nm. The normalized output power in the bar and cross ports are plotted as a function of index modulation in Fig. 3. The

#82652 - $15.00 USD Received 2 May 2007; revised 28 Jun 2007; accepted 29 Jun 2007; published 6 Jul 2007

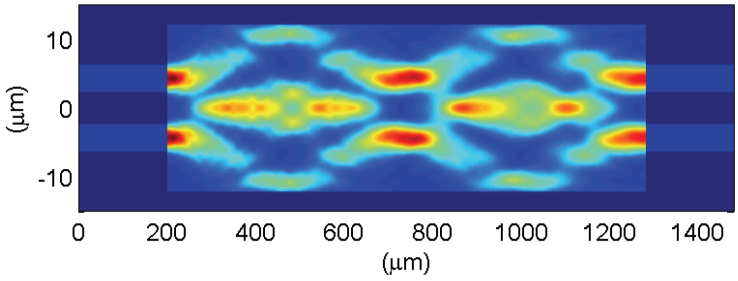

Fig. 2. Calculated hologram for variable splitting ratio 2×2 MMI coupler using wide-angle beam propagation method (WA-BPM).

two curves in the same figure are theoretical fits with Eq.(8) and Eq.(9). Excellent agreement between the matrix theory and WA-BPM simulations can be seen in the figure. An effective index modulation of -0.002 is required for a full swing of the power splitting ratio at the output ports. Using the effective index method, it is found that a Δn of -0.002 can be obtained by surface relief patterns etched into the multimode section of the MMI with a depth of approximately 300nm.

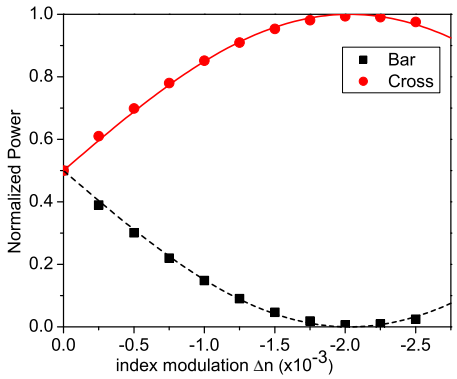

Fig. 3. Simulated bar port and cross port outputs with different index modulation on MMI. Curves are theoretical fits calculated from Eq.(8) and Eq.(9).

4.2. Wavelength dependence of MMI power splitter with hologram

We define R as the ratio between bar port output intensity and cross port output intensity. Using power splitters designed and optimized for operation at 1550nm, we vary the input wavelengths from 1500nm to 1600nm in increments of 10nm to investigate wavelength dependence of these devices. We define the difference between R and the designed value at 1550nm, R_{1550}, as ΔR. These variations for a 50:50 MMI splitter without holograms, along with three hologram-loaded MMIs with index modulations of -0.0005,-0.0010,-0.0015 are normalized against the designed value R_{1550} and shown in Fig. 4. It can be seen that the spectral variations in the power splitting ratios of hologram-loaded MMIs are comparable to that of the MMI splitter without holograms. We also plot the normalized total transmittance of these devices as a function of wavelength in Fig. 5. Transmittance decrease as wavelength is detuned from the design wavelength. As

#82652 - $15.00 USD Received 2 May 2007; revised 28 Jun 2007; accepted 29 Jun 2007; published 6 Jul 2007

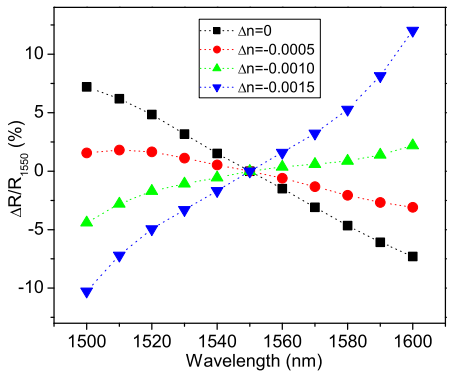

Fig. 4. Simulated variation in power output ratio between bar and cross ports with respect to input wavelength. The variations are normalized with the ratio at the designed wavelength of 1550nm.

expected, excess loss is observed when index modulation is increased. Overall, the devices exhibit excellent power splitting performance and high transmittance over a wide bandwidth of 100nm.

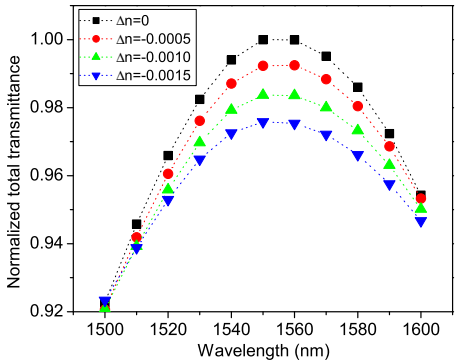

Fig. 5. Simulated total transmittance with respect to input wavelength.

5. Fabrication tolerance

The fabrication tolerance of these devices can be addressed separately for the hologram and the MMI. Errors in the hologram etching depth, d_{etch}, is directly related to errors in the effective index modulation, Δn, which affects the power splitting ratio as shown in Fig. 3. For our design example, since d_{etch} and Δn follow a linear relation, the sensitivity of power splitting ratio to d_{etch} is thus the slope of the curves in Fig. 3. We consider a d_{etch} error of 30nm (corresponding Δn error of 0.0002) and calculate its effect on the power splitting ratio. The maximum error is found for the 50:50 splitter (maximum slope) with a resulting splitting ratio of 57.8:42.2; while

#82652 - $15.00 USD Received 2 May 2007; revised 28 Jun 2007; accepted 29 Jun 2007; published 6 Jul 2007

the minimum error is found for the 100:0 splitter (minimum slope) with a resulting splitting ratio of 99.4:0.6. For fabrication errors in the MMI, such as the width, W_{mmi}, due to undercutting from the etching process, the optimal operating wavelength will be changed for the designed MMI length as can be seen in Eq. (1). In this case, the hologram design is no longer optimal at the original designed wavelength. The hologram basically consists of multiplexed long-period gratings with grating periods defined by the differences between the propagation constants of the modes of the multimode section [7]. From Eq. (18) in [1], we know that the difference in propagation constants between two modes j and k can be expressed as

$$\mathbf{k}_{jk} = \frac{\pi\lambda}{4n_c W_e^2}(j^2 - k^2). \tag{10}$$

As a result, as long as the condition in Eq. (1) is satisfied at the new optimal wavelength, the grating period defined in Eq. (10) will be satisfied as well. In other words, the designed hologram is now optimal at a new wavelength as a result of the MMI fabrication error. We expect the device to show a similar spectral dependence to the ones shown in Figs. 4 and 5 but centered at the new optimum wavelength.

6. Summary

We have demonstrated the feasibility of generating arbitrary power splitting ratios with multimode waveguide holograms on 2×2 MMI couplers. The principle of hologram design using self-imaging properties is extended for the case of paired-interference and can be applied to any intermediate imaging planes. The same principle can be used to design $N \times N$ power splitters or interconnects with new splitting ratios.

Based on the new design principle, variable 2×2 power splitters are designed using SOI rib waveguide structures. These devices should have good performance over a bandwidth of 100nm as shown by beam propagation simulations.

Acknowledgments

This material is based upon work supported in part by the STC Program of the National Science Foundation under Agreement Number DMR-0120967 and by a DARPA program.

#82652 - $15.00 USD Received 2 May 2007; revised 28 Jun 2007; accepted 29 Jun 2007; published 6 Jul 2007